Density-functional-based construction of transferable nonorthogonal tight-binding potentials for B, N, BN, BH, and NH

J. Widany, Th. Frauenheim, and Th. Köhler
Technische Universität, Institut für Physik, D - 09107 Chemnitz, Germany

M. Sternberg
Case Western Reserve University, Department of Physics, Cleveland, Ohio 44106

D. Porezag, and G. Jungnickel
Technische Universität, Institut für Physik, D-09107 Chemnitz, Germany

G. Seifert
Technische Universität, Institut für Theoretische Physik, Mommsenstrasse 13,D - 01062 Dresden, Germany
(Received 3 August 1995; revised manuscript received 29 September 1995)

We present a non-self-consistent density-functional based construction of nonorthogonal tight-binding (TB) matrix elements for B, N, BN, BH, and NH within the framework of the linear combination of atomic orbitals formalism using the local-density approximation. Despite the simplicity of the scheme considering only two-center Hamiltonian integrals and overlap matrix elements, the method has been proven to be sufficiently accurate and transferable to all scale BN(H) structures from small clusters and molecules to crystalline solids and solid surfaces. The calculation of forces is straightforward and allows an application of the method to molecular-dynamics simulations of structure formation in complex boron nitride systems.

I. INTRODUCTION

Boron nitride (BN) has become a material of considerable importance to semiconductor industry and to materials science. Due to its fascinating properties, such as extreme hardness, high melting point, chemical inertness, high thermal conductivity, large band gap, etc., cubic boron nitride (c-BN) films have a growing potential for many applications in modern electronic devices and for fabrication of protective coatings. BN as the lightest III-V semiconductor is isovalent to carbon and exists in different crystalline phases, the properties of which have been studied in great detail, both experimentally and theoretically. For a selected review, see Refs. 1–3. While the hexagonal structure h-BN, which apart from the different stacking AA' is isostructural to graphite, is claimed to be the normal stable phase at room temperature,[4] the cubic phase c-BN (zinc-blende structure) has been synthesized successfully in the laboratory under pressure.[5,6] While amorphous BN may exist[7] in chemical vapor or sputter deposited material, all experimental efforts are directed towards a low-temperature, low-pressure growth of c-BN films.

While experimental studies of the nucleation and growth of c-BN have proved highly successful, fundamental understanding of such processes is still rather poor. In recent years, *first-principle's* calculations within the Hartree-Fock,[8] the local-density-functional theory (LDF),[9–13] and *ab initio* calculations using ultrasoft pseudopotentials[14] have provided consistent results for the crystalline phase transformations under pressure, the ground-state optoelectronic and mechanical properties and the electronic band structure. However, there are no efficient empirical potentials or tight-binding schemes available for molecular dynamics to study the dynamic structure formation in bulk systems or on growing surfaces.

The required method should be simple, efficient, and provide simultaneously almost the same accuracy and transferability as the computationally more time demanding self-consistent field (SCF) density-functional (DF) methods. Recently, there has been considerable effort in developing parametrized orthogonal and nonorthogonal tight-binding (TB) schemes for several semiconductors.[15–21] The orthogonal schemes fail to provide a sufficient, transferable potential, that works well from few-atom clusters and molecules to the condensed solid without any inclusion of additional coordination-dependent parameters (like bond-counting terms and embedding energy functions).[16,22] Nonorthogonality is believed to improve the transferability.[23,24] However, even in the best tested empirically parametrized schemes, the accuracy compares unfavorably with results from *ab initio* calculations. Moreover no transferable TB scheme for complex BN systems exists in literature.

Therefore, we present results of a density-functional based construction of TB Hamiltonian and overlap matrices using atomic orbitals and potentials from LDF calculations of slightly contracted (pseudo) atoms. As in usual TB *Ansätzes*, only two-center Hamiltonian matrix elements are treated. The short-range repulsive part of the total potential still needs to be adjusted to SCF LDA data of proper reference systems. Despite its simplicity, the method has been proven to be sufficiently accurate and transferable to all-scale BN structures, including hydrogenated systems.

The outline of the paper is as follows. In Sec. II, we briefly characterize the density-functional method for the construction of nonorthogonal tight-binding parameters. In

Sec. III we summarize all tests performed for simulations on small clusters, molecules, and solid-state modifications. Comparing experimental data and *ab initio* calculations with the data derived within our method, we find a reasonable overall agreement. In Sec. IV, a list of problems will be outlined for current applications, the study of which may provide a better understanding of the c-BN formation.

II. DENSITY-FUNCTIONAL TIGHT-BINDING METHOD FOR B-B, N-N, B-N AND B-H, N-H

The method for calculations of the total energy and the interatomic forces is based on a non-self-consistent density-functional scheme within the linear combination of atomic orbitals LCAO framework using the local density approximation. For details we refer the reader to a recently published paper.[21]

In contrast to most empirical TB schemes the Hamiltonian and overlap matrix elements are not obtained from a fit to an experimental database but are derived in the following way. For each atom type, the eigenfunctions of appropriately constructed pseudoatoms are determined. As in the paper by Porezag *et al.*,[21] we used $r_0 = 1.48$ Å for boron, $r_0 = 1.38$ Å for nitrogen and $r_0 = 0.69$ Å for hydrogen as parameters of the additional potential $\sim (r/r_0)^2$ thus confining the range of the valence electron orbitals in the self-consistent single-atom calculations.

The confinement radius r_0 is related to the covalent radius of the particular atom type and does not involve further parametrization. The corresponding contracted eigenfunctions are then used as a basis set to represent the wave functions of the many-atom structures. Neglecting three-center and crystal field integrals, we calculate all necessary matrix elements in a straightforward manner using LDF theory. Since this approximation leads to matrix elements (Slater-Koster integrals) that depend only on internuclear distances, it is possible to parametrize the Hamiltonian as in empirical TB models. After solving the general eigenvalue problem for the determination of the single-particle energies and eigenstates of the system, the total energy is written as a sum of a ''band-structure energy'' (sum of occupied Kohn-Sham energies) and a repulsive two-particle interaction. Following Ref. 21, this repulsive energy is derived as a universal short-range pair potential from adjusting the difference between the band-structure energy of the diatomics B-B, N-N, B-N, H-H, B-H, N-H, and the corresponding SCF-LDA cohesive energy curves. To obtain the B-N repulsive potential, we have included the SCF crystalline data[25] of the c-BN cohesive energy curve around the equilibrium bond length as additional reference points.

In Figs. 1(a)–1(h) we have plotted the Hamiltonian and overlap matrix elements versus interatomic separation for B-B, N-N, B-N, B-H, N-H, and H-H.[26] In Fig. 2 we show the corresponding analytically fitted short-range repulsive two-particle potentials.

III. TESTS AND RESULTS

A. Small clusters

In the following we present the results of tests performed on small homonuclear and heteronuclear B_nN_m clusters, $n,m \leqslant 3$. As outlined in Table I, we discuss the relative energetic stability of various clusters and compare geometrical parameters, vibrational frequencies, and Mulliken charge distributions of the most stable clusters with *ab initio* results.[27]

To enable comparision with various *ab initio* calculations and experiments we have corrected the LDA binding energies by the spin polarization energies of the free B and N atoms of 0.24 and 2.91 eV, respectively. For B_2 and N_2 we obtain binding energies of 3.47 and 11.62 eV in reasonable agreement with *ab initio* calculations (3.15 and 9.91 eV) (Ref. 27) and experimental data (3.08 and 9.90 eV).[28] For the BN diatomic we find a binding energy of 6.45 eV, which is close to the SCF value, 6.36 eV (Ref. 29) rather than 4.42 eV as obtained by *ab initio* methods.[27]

B_3: In agreement with high level *ab initio* calculations [HF plus many-body perturbation treatment - MP3 (Ref. 27)] the most stable configuration has been found to be the equilateral triangle. While the bond length almost matches the *ab initio* value the vibrational frequencies are overestimated up to about 25%. The large mismatching, particularly, in the low-frequency modes but also deviations of about 25% in the high-frequency numbers found between *ab initio* and DF-TB calculations are within the uncertainty of the chosen basis sets and approximations schemes. The linear chain is found as a metastable configuration at considerable higher energy, + 1.18 eV.

B_2N: Substituting one boron by nitrogen, the symmetric linear chain cluster becomes the most stable one. Again, the geometric parameters agree well with the *ab initio* data and the vibrational frequencies are reasonable. The very soft bending mode found by *ab initio* calculations[27] at 82 cm^{-1} in the present calculation occurs at 181 cm^{-1}. The Mulliken charge distribution shows a charge transfer from the central nitrogen atom to the boron atoms on each side. The B-B-N-configuration with bond lengths of 1.644 and 1.256 Å is found to be metastable, with an energy 0.066 eV higher than the B-N-B structure.

BN_2: Due to the occurrence of a number of low-lying electron states, the situation for this cluster is rather complex. The isosceles triangle has been determined to be 0.1 eV more stable than the asymmetric linear chain by *ab initio* calculations using different basis sets and considering the electron correlation on the MP4 level.[27] In contrast to the DF-TB scheme we find the linear chain to be 1.85 eV lower in energy than the triangle. For these two configurations we obtain also the strongest deviations from the *ab initio* geometries. However, the vibrational frequencies and the Mulliken charges are described fairly well. The symmetric linear chain as a third metastable cluster by 2.04 eV is higher in energy than the asymmetric linear chain.

N_3: Comparing all possible configurations the symmetric linear N_3 chain is established as the ground state in agreement with *ab initio* data. This geometry is about 4.1 eV lower in energy than the isosceles triangle. The obtained bond length of 1.192 Å is closer to the experimental value of 1.1815 Å (Ref. 30) than the *ab initio* value.

B. Molecules

Many stable molecules containing hydrogen, boron, and nitrogen are known. These molecules are of interest for de-

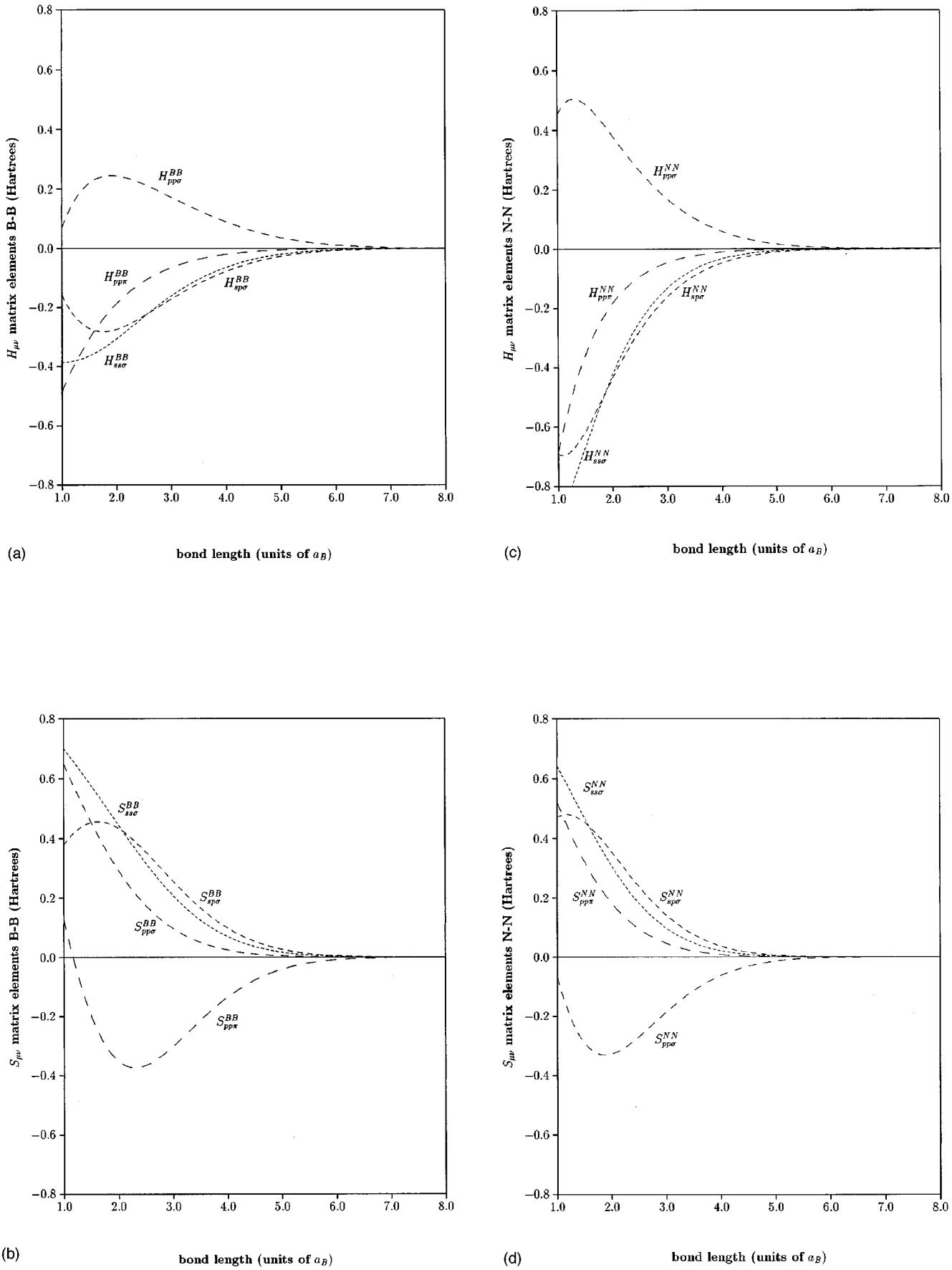

FIG. 1. (a)–(h) Hamiltonian and overlap matrix elements versus interatomic separation: (a) $H_{\mu\nu}$(B-B), (b) $S_{\mu\nu}$(B-B), (c) $H_{\mu\nu}$(N-N), (d) $S_{\mu\nu}$(N-N), (e) $H_{\mu\nu}$(B-N,N-B), (f) $S_{\mu\nu}$(B-N,N-B), (g) $H_{\mu\nu}$(B-H,N-H,H-H) and (h) $S_{\mu\nu}$(B-H,N-H,H-H).

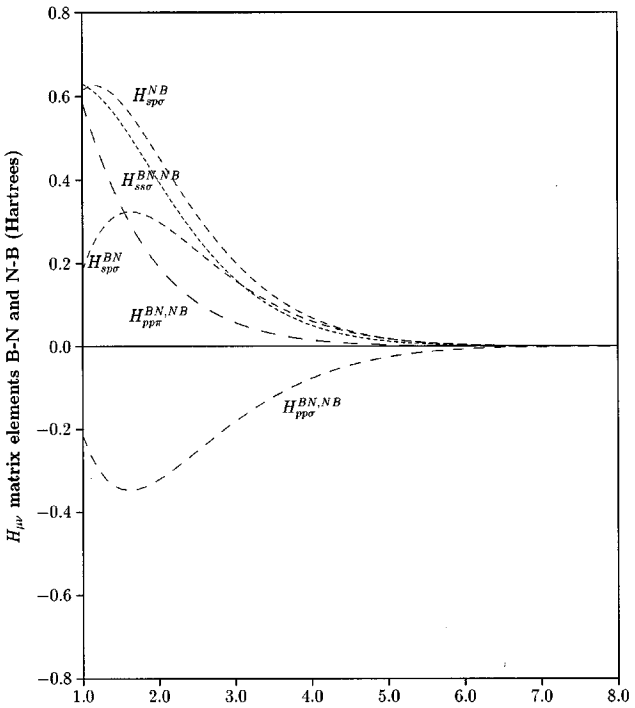

(e)

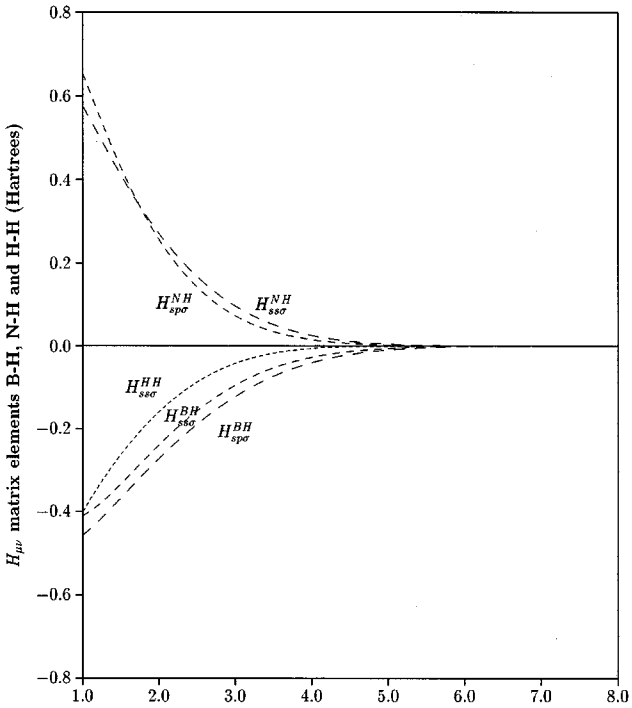

(g)

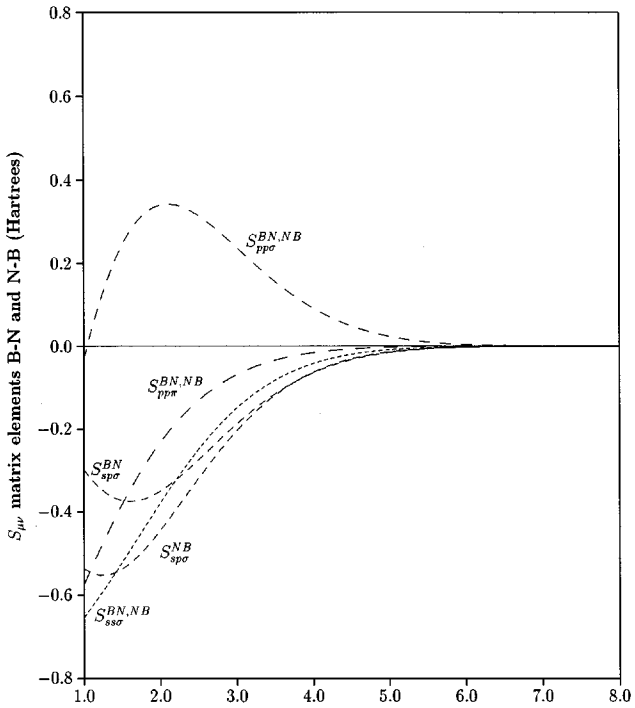

(f)

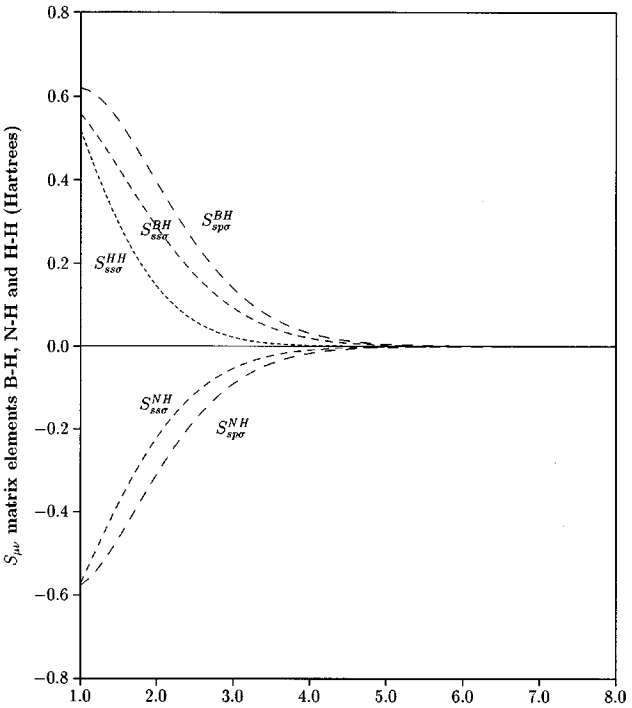

(h)

FIG. 1 (*Continued*).

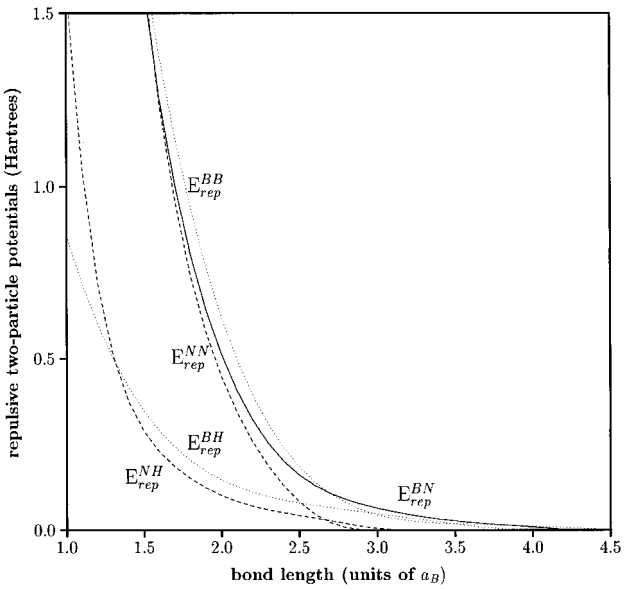

FIG. 2. Short-range repulsive two-particle potentials vs interatomic separation for different atom combinations.

scribing the agglomeration of clusters and growth on crystalline substrates. We have tested various molecules that are well characterized from both theory and experiment and prove the reliability of the method to describe properly the different types of B-N bonding. For comparison of molecular systems we refer to *ab initio* calculations on the HF level,[31–35] to *semiempirical* modified neglect of differential overlap (MNDO) calculations[36] and experiments.[37–39] The geometrical parameters of the optimized molecule configurations are summarized in Table II. We also discuss the phonon frequencies and the Mulliken charge distribution (shown in Table III) for selected molecules.

Iminoborane (HBNH): The bonding situation in the iminoborane can be considered to incorporate both the B and N atoms in a sp-hybridizated state. We found a B-N bond length at 1.234 Å, indicating a strong B-N bond, in very good agreement with MNDO and *ab initio* SCF molecular orbital (MO) calculations [1.233 (Ref. 31) and 1.23 Ref. 40)]. It may be characterized as a triple bond, corresponding to a rather large B-N overlap population ($P_{(\mathrm{B-N})}=1.5$). The Mulliken charge analysis also compares well with MO calculations on the STO-3G level.[41]

The amino group in amino-iminoborane [$HNBNH_2$] is found to be planar. The NBN bond angle is close to 180°. The lengths of the BN(1) bond with 1.264 Å and the overlap population with 1.3 are nearly the same as in iminoborane, hence it may also be viewed as a triple bond. The BN(2) bond length (1.400 Å) is clearly shorter than a B-N single bond ($\sim$1.5 Å), and the bond (overlap population $P_{(\mathrm{N-B})}=0.9$) can be characterized nearly as a double bond. These results are in close agreement with the results from *ab initio* calculations.[36,41]

Aminoborane [H_2BNH_2]: Aminoborane as the fundamental structure unit of alternating unsaturated boron-nitrogen compounds has received much experimental and theoretical attention. The BN bond length obtained with 1.359 Å is a little bit shorter than the BN(2) bond length in amino-iminoborane and fits the double bond value (1.36 Å), whereas the overlap population is slightly larger than that between B and N(2) in amino-iminoborane. The planarity of the molecule and the HNB and HBN bond angles that both come close to 120° are characteristic for sp^2 hybridization of the boron and nitrogen atoms. Our bond lengths and angles agree well with both *ab initio* HF calculations[32,34] and experimental values.[37]

TABLE I. Minimal energy B_nN_m clusters, $n,m \leqslant 3$. Binding energies in eV, bond lengths in Å, bond angles in degrees, Mulliken charge distribution (MCD) and vibrational modes in cm^{-1}.

Cluster	Symm.		Present work	*Ab initio* results[27]
B_3	D_{3h}	E_B	9.56	8.764
		r_{BB}, Θ_{BBB}	1.588, 60.0	1.5742, 60.0
		Q_B	0.00	0.00
		ν	1068, 1068, 1645	972, 972, 1217
B_2N	$D_{\infty h}$	E_B	11.68	11.703
		r_{BN}	1.312	1.3089
		Q_B,Q_N	0.115, −0.230	0.209, −0.418
		ν	181, 181, 1349, 1739	82, 82, 1245, 2271
BN_2	C_{2v}	E_B	10.49	9.998
		r_{BN}, r_{NN}, Θ_{NBN}	1.448, 1.362, 56.6	1.3947, 1.2665, 54.0
		Q_B, Q_N	0.188, −0.094	0.305, −0.153
		ν	977, 1082, 1545	1221, 1290, 1760
BN_2	$C_{\infty v}$	E_B	12.34	9.777
		r_{BN}, r_{NN}	1.374, 1.140	1.4217, 1.1449
		Q_B, Q_{N1}, Q_{N2}	−0.473, 0.513, −0.040	0.033, −0.137, 0.105
		ν	247, 1181, 1933	255, 935, 1622
N_3	$D_{\infty h}$	E_B	14.01	9.361
		r_{NN}	1.192	1.1593
		Q_{N1},Q_{N2},Q_{N3}	−0.454, 0.909, −0.454	−0.193, 0.386, −0.193
		ν	448, 449, 1340, 1383	530, 679, 1504, 1703

TABLE II. Geometrically optimized molecule configurations: bond lengths in Å, angles in degrees.

Molecule Symm.	Method	Parameter	Geometrical data
HBNH	Present work	HB, BN, NH	1.199, 1.234, 1.028
$D_{\infty v}$	*Ab initio* results[31]		1.167, 1.233, 0.989
$HNBNH_2$	Present work	HN, NB, BN, NH, HNH	1.029, 1.264, 1.400, 1.035, 114.7
C_{2v}	*Ab initio* results[36]		0.967, 1.189, 1.382, 0.990, 118.8
H_2BNH_2	Present work	HB, BN, NH, HBN, BNH	1.217, 1.359, 1.036, 120.2, 123.7
C_{2v}	*Ab initio* results[34]		1.187, 1.391, 0.994, 119.7, 123.9
	Expt. results[37]		1.184, 1.403, 1.003, 120.7, 118.2
$HB(NH_2)_2$	Present work	HB, BN, NH, HNB, NBN	1.217, 1.411, 1.034, 122.9, 122.3
C_{2v}	*Ab initio* results[32]		1.193, 1.424, 1.006, 122.7, 122.3
	Expt. results[38]		1.193, 1.418, 1.005, 123.7, 122.0
$HN(BH_2)_2$	Present work	HN, NB, BH, HBN, BNB	1.046, 1.434, 1.217, 120.5, 124.5
C_{2v}	*Ab initio* results[32]		1.006, 1.435, 1.193, 119.5, 126.5
$(\text{-BH-NH-})_3$	Present work	BH, BN, NH, NBN, BNB	1.216, 1.423, 1.035, 117.6, 122.3
D_{3h}	*Ab initio* results[35]		1.187, 1.430, 0.994, 117.5, 122.5
	Expt. results[39]		1.258, 1.436, 1.050, 117.5, 121.1

Diaminoborane $[HB(NH_2)_2]$, and trisaminoborane $[B(NH_2)_3]$: The geometrical parameters for these molecules as well as for diborylamine $[HN(BH_2)_2]$, and trisborylamine $[N(BH_2)_3]$, which are obtained by cyclic substitution of B and N atoms are in very good agreement with both theoretical[32,33] and experimental values,[38] compare Table II.

Borazin $[(\text{-BH-NH-})_3]$: This molecule is isoelectronic to benzene and therefore sometimes called ''inorganic benzene.'' We obtained a planar structure with a BN bond length of 1.423 Å. This is in excellent agreement with both *ab initio* SCF MO calculations [1.429 Ref. 36 and 1.430 Å (Ref. 35)] and experimental values [1.436 Å (Ref. 39)]. In contrast to HF calculations we find a rather small charge transfer from boron to nitrogen, which resembles more to the benzene molecule that seems to be more reasonable than the strong charge alternations as obtained in Ref. 35. The B-N overlap populations show no bond alternations, i.e., the populations between each neighboring atom are the same and have a value comparable to that between B and N(2) in amino-iminoborane.

To test the dynamical properties of our potential, we have also determined the phonon frequencies for a number of molecules. Since there are no systematic experimental data and only limited theoretical investigations at hand we choose aminoborane as a representative for comparision. Considering the frequencies of the various types of modes as listed in Table IV, we obtain fair agreement with the experimentally reported frequencies.[43] As with the MNDO calculations[42] the BH and BN stretching modes are overestimated by about 20%.

C. Solid

Though there are accurate self-consistent LDA results on cohesive energies and bulk modulus available for various modifications of boron nitride,[13,14] no applications of *ab initio*[44,45] and generalized tight-binding[17] molecular dynamics have been made so far to our knowledge to study the structure formation in BN systems.

Since we want to address possible applications to crystalline structures and substrate surfaces we have performed calculations of the total energy versus nearest-neighbor distance for the crystalline modifications *h*-BN, *c*-BN, and the high-pressure rocksalt structure. The calculations make use of a Γ-point Brillouin sampling, a valid approximation for large enough supercells. The results compared to the *ab initio* data

TABLE III. Mulliken charge distribution of molecule configurations. (H_N denotes the hydrogen attached to the nitrogen).

Molecule	Method	Mulliken charge distribution	
HBNH	Present work	Q_{H_B}, Q_B, Q_N, Q_{H_N}	0.05, 0.06, −0.38, 0.27
	Ab initio results[41]		0.03, 0.29, −0.48, 0.31
$HNBNH_2$	Present work	Q_{H_N}, Q_N, Q_B, Q_N, Q_{H_N}	0.28, −0.62, 0.33, −0.41, 0.21
	Ab initio results[41]		0.20, −0.51, 0.45, −0.53, 0.19
H_2BNH_2	Present work	Q_{H_B}, Q_B, Q_N, Q_{H_N}	−0.08, −0.05, −0.12, 0.20
	Ab initio results[32]		−0.07, 0.36, −0.88, 0.33
$HB(NH_2)_2$	Present work	Q_{H_B}, Q_B, Q_N, Q_{H_N}	−0.09, 0.11, −0.41, 0.20
	Ab initio results[32]		−0.09, 0.70, −0.94, 0.32
$(\text{-BH-NH-})_3$	Present work	Q_{H_B}, Q_B, Q_N, Q_{H_N}	−0.09, 0.14, −0.24, 0.19
	Ab initio results[35]		−0.08, 0.88, −1.15, 0.35

TABLE IV. Harmonic frequencies of aminoborane in cm^{-1}.

Assignment	Present work	Calc. MNDO frequency[42]	Corr. MNDO frequency[42]	Expt. frequency[43]	Type
a_1	3447	3660	3416	3460	NH stretch
	2938	2915	2530	2445	BH stretch
	1698	1792	1663	1613	NH_2 scissor
	1623	1516	1345	1342	BN stretch
	1173	1321	1192	1130	BH_2 scissor
b_2	3344	3643	3399	3333	NH Stretch
	3004	2968	2583	2525	BH stretch
	1227	1207	1061	1105	NH_2 rock
	788	850	704	738	BH_2 rock
a_2	896	813	789	IR inactive	NH_2-BH_2 twist
b_2	502	621	621	690	NH_2 out of plane
	903	1108	936	962	BH_2 out of plane

of Xu and Ching,[2] Wentzcovitch and co-workers[10,11,13] and Furthmüller, Hafner, and Kresse[14] are displayed in Table V. Whereas Furthmüller, Hafner, and Kresse[14] predict the close-packed c-BN phase to be more stable than the layered h-BN phase by 0.055 eV/atom, we obtain the hexagonal modification as the most stable one in agreement with Xu and Ching.[2] Wentzcovitch and co-workers[12,13] reported c-BN to be more stable than layered rhombohedral r-BN by about 0.06 eV/atom. The fact that the calculated energies for h-BN and r-BN are almost equal, as discussed in Ref. 13, indicates that the LDA is inadequate in properly describing the interlayer bonding. LDA is likely to underestimate the cohesion in the layered phases because the charge density in the interplanar region is very small. Beyond this, the inclusion of the zero-point energies will compensate for the calculated energy difference between r-BN and c-BN. Within the the numerical accuracy, the two calculated energies are practically the same. The high-pressure rocksalt structure in our calculation is found as a third metastable modification lying 1.79 eV/atom above the c-BN in very good agreement with the SCF values.

We calculated the electronic band structures for the hexagonal, the wurtzite, and the zinc-blende phases of boron nitride. The data were obtained in the usual way: setting up a Bloch sum over the pseudoatom orbitals and calculating the Kohn-Sham eigenvalues for a series of wave vectors along lines of high symmetry in the Brillouin zone. We find that our valence-band structures agree with a number of more sophisticated methods.[2,10,14,46–50] The three solid-state structures are found to have a gap at the Fermi level. However, the method is not capable of reproducing the conduction bands correctly, which is a consequence of the usage of a minimal basis. In all three cases we find a direct band gap instead of a indirect one as obtained in self-consistent studies. For the hexagonal phase, this is in agreement with an empirical TB investigation.[51]

The analysis of the Mulliken charge distribution in hexagonal as well as in cubic BN gives a rather strong charge transfer from nitrogen to boron ($q_{B/N}=\pm 0.327$ in h-BN, $q_{B/N}=\pm 0.285$ in c-BN). Interestingly, the charge transfer is a little bit larger in h-BN than in c-BN. The BN overlap population (P_{BN}) is larger in h-BN ($P_{BN}=0.78$) than in

TABLE V. Cohesive and structural properties of different BN lattice types: cohesive energy E_0 (obtained with respect to the spin-unpolarized boron and nitrogen atoms), structural energy difference ΔE relative to the zinc-blende structure and lattice constant a.

Structure	Present work	Ref. 2	Refs. 10 and 11	Ref. 14
		Zinc-blende		
E_0 (eV/atom)	−7.77	−7.00	−7.15	−8.152
ΔE (eV/atom)	0.00	0.00	0.00	0.00
a (Å)	3.671	3.615	3.606	3.576
		Hexagonal		
E_0 (eV/atom)	−7.90	−7.35		−8.097
ΔE (eV/atom)	−0.13	−0.35	+0.06 [a]	+0.055
a (Å)	2.50	2.49		2.486
		Rocksalt		
E_0 (eV/atom)	−5.98		−5.45	−6.429
ΔE (eV/atom)	+1.79		+1.70	+1.723
a (Å)	3.84		3.49	3.458

[a]Data obtained for rhombohedral r-BN.

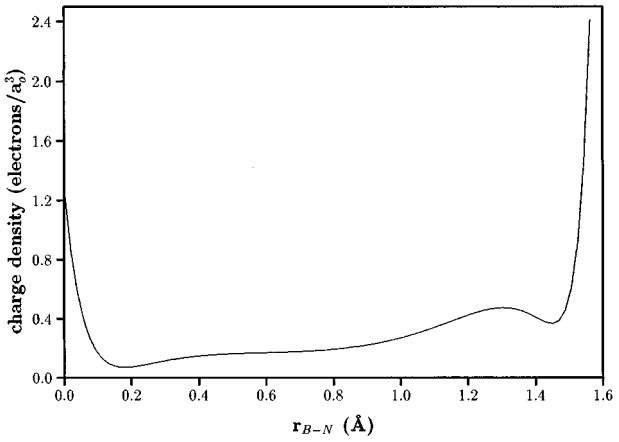

FIG. 3. Charge density distribution along the BN bond in *c*-BN.

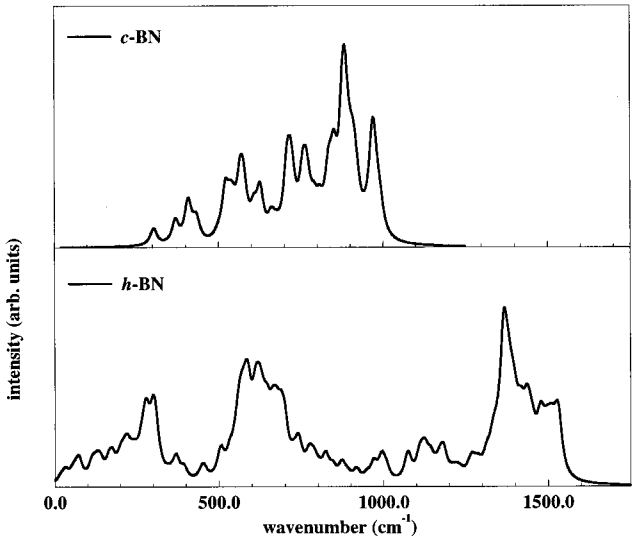

FIG. 4. Vibrational density of states for *c*-BN and *h*-BN. The eigenvalues are broadened with Lorentzians of 40-cm^{-1} width.

c-BN ($P_{BN}=0.59$), as expected. The B-N overlap population as well as the B-N interatomic distance agree very well with that in borazine. That means the B-N bond in *h*-BN is very similar to that in borazine. Cubic BN has the smallest B-N overlap population and the largest interatomic distance of all the three crystalline forms. The B-N bond in *c*-BN may be characterized as a long single bond. However, in the evaluation of the strength of the bonding one has to consider that the coordination number for each atom is increased from three to four, going from *h*-BN to *c*-BN. Interestingly, multiplying the B-N overlap population in *c*-BN with 4/3 one obtains nearly the value of the B-N overlap population in *h*-BN. In Fig. 3 the calculated valence charge density along the BN bond in *c*-BN is plotted. The results agree well with first-principles SCF LDA results.[2]

As an additional benchmark we have calculated the vibrational density of states for a *c*-BN 216-atom supercell and a *h*-BN 240-atom supercell. The resulting spectra agree well with vibrational densities of states obtained by SCF LDA supercell calculations.[52] Convoluting the vibrational spectra by a characteristic broadening function for neutron scattering the results compare nicely with recently obtained inelastic neutron data.[53] Figure 4 shows the spectra after broadening the eigenvalues with Lorentzians of 40-cm^{-1} width. A rough analysis of the modes reveals the following properties:

Cubic BN: The vibrational density of states of cubic boron nitride can be split into three main broad bands. The frequency region between 800 and 1000 cm^{-1} containing the most prominent peak centered at about 883 cm^{-1} is clearly occupied by B-N stretching vibrations. Compared to recent *ab initio* studies[52] the main peak is shifted to lower frequencies by about 12%. In comparision with experimental data we find an underestimation of the TO peak (1054 cm^{-1}) (Ref. 55) by about 15%. Towards decreasing energies we can assign bending vibrations in the spectrum between $\sim$ 500 and 800 cm^{-1}. The dominating part of the modes appears to be composed of coupled excitations. The lowest weak band feature below 500 cm^{-1} is dominated by mostly translational motions of B-N units within the grid.

Hexagonal BN: The spectra are decomposed into two main regions. The high-frequency bands between 1300 and 1600 cm^{-1} are again occupied by various kinds of B-N stretching vibrations. While the intense and sharp peak centered at about 1370 cm^{-1} is dominated by B-N stretching of entire rings, the shoulder at higher frequencies with a relative sharp cutoff at 1550 cm^{-1} can be attributed to symmetric and asymmetric stretching between neighboring B-N zigzag chains. These results are in very good agreement with experimental findings,[55] where a Raman-active mode appears at 1370 cm^{-1} and two IR active modes are found at 1367 and 1610 cm^{-1}. The weak feature between 1000 and 1200 cm^{-1} represents another possible stretch mode. Here, the central atom (B or N) rests, while the three adjacent neighbors of opposite type perform a symmetric stretching motion. Below 900 cm^{-1} we find mostly out-of-plane-type excitations. The heteronuclearity is responsible for the gaplike intensity drop at about 420 cm^{-1}. The out-of-plane vibrations of boron occur at higher frequencies than that of the nitrogen ones. This is clearly indicated by separated broad bands within this region.

IV. SUMMARY

We have presented a scheme for the determination of Hamiltonian and overlap matrix elements on the basis of density-functional theory in the framework of a method similar to widely used nonorthogonal empirical tight-binding schemes. Only two-center Hamiltonian integrals are incorporated, completely neglecting three-center and crystal field integrals in the calculations. The usual short-range repulsive interaction appearing in TB models is fitted as a universal two-particle potential to self-consistent data derived in LDA. Despite its extreme simplicity, the potential is highly transferable without additional changes to the total energy expression and gives reliable results for geometries, cohesive energies, and vibrational modes for all-scale BN-H structures, ranging from small clusters through molecules to solid-state

modifications. On this basis we address future applications of DF-TB molecular dynamics to investigations of the reconstruction behavior and growth on various *c*-BN surfaces and studies of interfaces in relation to homoepitaxial and heteroepitaxial growth. In particular, the stable and metastable surface reconstructions on *c*-BN (100), (110), and (111) at different atom type termination are currently under investigation.[56] Furthermore, investigations concerning the *h*-BN–*c*-BN interface in support of recent experimental findings[57,58] may provide additional insight into the *c*-BN nuclation.[59]

ACKNOWLEDGMENTS

We gratefully acknowledge support from the Deutsche Forschungsgemeinschaft and the trinational D-A-CH cooporation.

[1] L. Vel, G. Demazeau, and J. Etourneau, Mat. Sci. Eng. B **10**, 149 (1991).
[2] Y.-N. Xu and W. Y. Ching, Phys. Rev. B **44**, 7787 (1991).
[3] R. C. DeVries, in *Diamond Films and Diamond-Like Films and Coatings*, edited by R. E. Clausing *et al.* (Plenum, New York, 1991).
[4] R. S. Pease, Acta Crystallogr. **5**, 536 (1952).
[5] F. P. Bundy and R. H. Wentorf, J. Chem. Phys. **38**, 1144 (1963).
[6] G. Demazeau, Diamond Relat. Mater. **4**, 284 (1995).
[7] B. Rother, Chr. Weissmantel, H. D. Zscheile, C. Heiser, G. Holzhüter, G. Leonhardt, and P. Reich, Thin Solid Films **142**, 83 (1986).
[8] R. Dovesi, C. Pisani, C. Roetti, and P. Dellarole, Phys. Rev. B **24**, 4170 (1981).
[9] A. Zunger and A. J. Freeman, Phys. Rev. B **17**, 2030 (1978).
[10] R. M. Wentzcovitch, K. J. Chang, and M. L. Cohen, Phys. Rev. B **34**, 1071 (1986).
[11] R. M. Wentzcovitch, M. L Cohen, and P. K. Lam, Phys. Rev. B **36**, 6058 (1987).
[12] R. M. Wentzcovitch, S. Fahy, M. L. Cohen, and S. G. Louie, Phys. Rev. B **38**, 6191 (1988).
[13] P. K. Lam, R. M. Wentzcovitch, and M. L Cohen, Mat. Sci. Forum **54&55**, 165 (1990).
[14] J. Furthmüller, J. Hafner, and G. Kresse, Phys. Rev. B **50**, 15 606 (1995).
[15] C. Z. Wang, C. T. Chan, and K. M. Ho, Phys. Rev. B **39**, 8586 (1989).
[16] I. Kwon, R. Biswas, C. Z. Wang, K. M. Ho, and C. M. Soukoulis, Phys. Rev. B **49**, 7242 (1994).
[17] M. Menon and K. R. Subbaswamy, Phys. Rev. B **51**, 952 (1995).
[18] P. J. Ordejon, D. Lebedenko, and M. Menon, Phys. Rev. B **50**, 5645 (1994).
[19] J. L. Mercer and M. Y. Chou, Phys. Rev. B **49**, 8506 (1994).
[20] C. Molteni, L. Colombo, and L. Miglio, Phys. Rev. B **50**, 4371 (1994).
[21] D. Porezag, Th. Frauenheim, Th. Köhler, G. Seifert, and R. Kaschner, Phys. Rev. B **51**, 12 947 (1995).
[22] K. Laasonen and R. Nieminen, J. Phys. C **2**, 1509 (1990).
[23] M. Menon and K. R. Subbaswamy, Phys. Rev. B **47**, 12 754 (1993).
[24] L. M. Canel, A. E. Carlsson, and P. A. Fedders, Phys. Rev. B **48**, 10 739 (1993).
[25] J. L. Corkill, A. Y. Liu, and M. L. Cohen, Phys. Rev. B **45**, 12 746 (1992).
[26] The related Slater-Koster tables, parametrized using a distance mesh of $0.02a_B$ up to a cutoff of $10a_B$, are available upon request from the authors.
[27] J. M. L. Martin, J. P. Francois, and R. Gijbels, J. Chem. Phys. **90**, 6469 (1989).
[28] K. P. Huber and G. Herzberg, in *Constants of Diatomic Molecules* (Van Nostrand Reinhold, New York, 1979).
[29] G. te Velde and E. J. Baerends, J. Comput. Phys. **99**, 84 (1992).
[30] C. R. Baizer, P. F. Bernath, J. B. Burkhelder, and C. J. Howard, J. Chem. Phys. **89**, 1762 (1988).
[31] D. J. DeFrees, J. S. Binkley, and A. D. McLean, J. Chem. Phys. **80**, 3720 (1984).
[32] T. Fjeldberg, G. Gundersen, T. Jonvik, H. M. Seip, and S. Sæbø Acta Chem. Scand. A **34**, 547 (1980).
[33] G. Gundersen, Acta Chem. Scand. A **35**, 729 (1981).
[34] A. L. Hinde, A. Pross, and L. Radom, J. Comp. Chem. **1**, 118 (1980).
[35] R. J. Boyd, S. C. Choi, and C. C. Hale, Chem. Phys. Lett. **112**, 136 (1984).
[36] B. Maouche and J. Gayoso, Int. J. Quantum. Chem. **22**, 891 (1983).
[37] M. Sugie, M. Takeo, and C. Matsumura, Chem. Phys. Lett. **64**, 573 (1979).
[38] L. R. Thorne and W. D. Gwinn, J. Am. Chem. Soc. **104**, 3822 (1982).
[39] J. H. Callomon, E. Hirota, K. Kuchitsu, W. J. Lafferty, A. G. Maki, and C. S. Pote, in *Structure Data of Free Polyatomic Molecules*, edited by K. H. Hellwege and A. M. Hellwege, Landolt Börnstein, New Series, Group II, Vol. 7 (Springer, Berlin, 1976).
[40] N. C. Baird and R. K. Datta, Inorg. Chem. **2**, 17 (1972).
[41] H. Nöth, S. Weber, B. Rasthofer, Ch. Narula, and A. Konstantinov, Pure Appl. Chem. **55**, 1453 (1983).
[42] M. J. S. Dewar and M. L. McKee, J. Mol. Struct. **68**, 105 (1978).
[43] C. T. Kwon and H. A. McGee, Inorg. Chem. **9**, 2458 (1970).
[44] R. Car and M. Parinello, Phys. Rev. Lett. **55**, 2471 (1985).
[45] O. F. Sankey and D. J. Niklewski, Phys. Rev. B **40**, 3979 (1989).
[46] A. Cattelani, M. Posternak, A. Baldereschi, and A. J. Freeman, Phys. Rev. B **36**, 6105 (1987).
[47] K. T. Park, K. Terakura, and N. Hamada, J. Phys. C **20**, 1241 (1987).
[48] M. P. Surh, S. G. Louie, and M. L. Cohen, Phys. Rev. B **43**, 9126 (1991).
[49] X. Blase, A. Rubio, S. G. Louie, and M. L. Cohen, Phys. Rev. B **51**, 6868 (1995).
[50] P. Rodriguez-Hernandez, M. Gonzales-Diaz, and A. Munoz, Phys. Rev. B **51**, 14 705 (1995).
[51] J. Robertson, Phys. Rev. B **29**, 2131 (1984).
[52] K. Karsch and F. Bechstedt (unpublished).
[53] B. Kamitakahara *et al.* (unpublished).

[54] J. A. Sanjurjo, E. Lopez-Gruz, P. Vogel, and M. Cardona, Phys. Rev. B **28**, 4579 (1983).
[55] R. Geick, C. H. Perry, and G. Rupprecht, Phys. Rev. **146**, 543 (1966).
[56] J. Widany *et al.* (unpublished).
[57] D. J. Kester, K. S. Ailey, and R. F. Davis, Diamond Relat. Mater. **3**, 332 (1994).
[58] D. L. Medlin, T. A. Friedmann, P. B. Mirkarimi, P. Rez, M. J. Mills, and K. F. McCarty, J. Appl. Phys. **76**, 295 (1994).
[59] J. Widany and Th. Frauenheim (unpublished).